Anal. Bioanal. Electrochem., Vol. 3, No. 3, 2011, 302-315

Analytical & Bioanalytical Electrochemistry

Full Paper

Corrosion Behavior of Electrodeposited Zn-Ni, Zn-Co and Zn-Ni-Co Alloys

Ramesh S. Bhat[1], Udaya Bhat K[2], A. Chitharanjan Hegde[1,*]

[1]*Electrochemistry Research Laboratory, Department of Chemistry, Karnataka University, Surathkal Srinivasnagar - 575025, India*

[2]*Department of Metallurgy and Materials Engineering, National Institute of Technology Karnataka University, Surathkal Srinivasnagar - 575025, India*

* Corresponding author; Tel.: +91-9980360242; Fax: +91-824-2474033

E-Mail: achegde@rediffmail.com

Received: 6 March 2011 / Accepted: 7 June 2011 / Published online: 20 June 2011

Abstract- Zn-Ni, Zn-Co and Zn-Ni-Co alloy coatings were electrodeposited galvanostatically using sulphate bath, having THC as additive. The bath composition and operating parameters have been optimized by standard Hull cell method. The effects of current density (c.d.), pH on composition, thickness, hardness of the deposit were studied. Under all conditions of deposition, the bath followed anomalous type of codeposition with preferential deposition of less noble metal. Corrosion resistances of the coatings were measured by potentiodynamic polarization and Electrochemical Impedance Spectroscopy (EIS) method showed that under optimal conditions, the corrosion resistance of Zn-Ni-Co alloy coatings is approximately 20 times and 18 times better than Zn-Ni and Zn-Co alloys of same thickness. The Zn-Ni-Co coating under optimal c.d. (3.0 A dm^{-2}) was found due to its inherent high dielectric barrier, evidenced impedance signals. High partial c.d. for zinc in Zn-Ni-Co alloy system supports the possibility of a synergistic catalytic effect of Co on Fe and vice versa. X-ray diffraction study clearly indicates that improved corrosion resistance of ternary alloy is due to the change in the phase structure of the coatings, compared to binary alloys. Surface morphology and composition of the coatings were examined by using Scanning Electron Microscopy (SEM), interfaced with EDX facility, respectively. The ternary Zn-Ni-Co coating may thus replace the conventional Zn-Ni and Zn-Co coatings in a variety of applications.

Key words- Zn-Ni-Co Alloy, Corrosion Study, Zn-Ni-Co Alloy, XRD, SEM

1. INTRODUCTION

Electrodeposition of metals and alloys has become widely used in many industries, with distinct advantages compared to most other alloy coating technologies [1]. Electrodeposited binary Zn-M (Where M = Fe, Co or Ni) alloys, exhibit improved properties compared to pure Zn [2, 3]. Zn-Ni and Zn-Co coatings have been formed by DC plating [4-9,10]. Coatings of zinc with iron-group metals have been found useful for applications such as automotive body panels, where bright corrosion resistant steel is sought [8]. The Zn-Ni alloys obtained by electrodeposition processes, with the amount of nickel varying between 8% and 14% by weight, give corrosion protection and physical properties five to six times superior to that obtained with pure zinc deposits [11,12]. However, the binary Zn-Ni (8-20%) thin films, in this range of nickel content, have a rough, non-uniform and unattractive finish, so a brightener system must be developed to obtain bright deposits [13]. On the other hand, the electrodeposition of Zn-Co alloys is interesting because these alloys exhibit a significant higher corrosion resistance and better surface morphology than pure zinc [14-18]. Coatings with low Co content are less noble than steel, so that they represent a sacrificial type of coating. Those with high Co content are nobler than steel and provide a barrier type of protection [19].

The corrosion resistance of Zn-M alloys has been found to depend significantly on the concentration of M in the deposit [20]. The use of specific bath additives has also been found beneficial with respect to corrosion resistance, even for low contents of M [21]. It has been observed that the ternary alloy Zn-Ni-Co is characterized by enhanced corrosion resistance compared to the binary Zn-Ni and Zn-Co alloys [22-24]. Cadmium plating has been extensively used as a corrosion resistant coating on hard steel for various applications [25]. Kim et al. [26] recently developed an alkaline electrodeposition process to deposit good quality of Zn-Ni-Cd deposits with high Ni and Zn contents. The corrosion resistance of Zn-M alloys has been found to depend significantly on the concentration of M in the deposit [27].

The term anomalous codeposition (ACD) was coined by Brenner [28] to describe an electrochemical deposition process in which the less noble metal is deposited preferentially under most plating conditions. This behavior is typically observed in codeposition of iron-group metals, or in codeposition of an iron-group metal with Zn or Cadmium. In the deposition of Zn-Ni alloys, for example, adding either ion to the solution enhances the rate of deposition of the other metal [1]. The present work was aimed at comparative evaluation of Zn-Ni, Zn-Co and Zn-Ni-Co coatings, with emphasis on surface morphology, phase content, and corrosion resistance.

2. EXPRIMENTAL

Electroplating solutions were prepared from reagent grade chemicals and distilled water. Standard Hull cell of 267 mL capacity was used to optimize the bath constituents (1A cell current). All depositions were carried out at 303K. Polished mild steel panels were used as cathode (area 5 cm^2) and pure zinc plate having same exposed area was used as andode. Bath solutions were adjusted to pH 3.0 - 4.0 using dilute sulfuric acid. A PVC cell of 250 cm^3 capacity was used with cathode-anode space of ~5 cm. All depositions were carried out under common conditions of temperature and duration of 10 minutes for the purpose of comparison. Depositions were carried out galvanostatically using sophisticated power source (N6705A, Agilent Technologies). The corrosion behavior of the coatings was measured by electrochemical DC and AC techniques. All electrochemical tests were carried out using Potentiostat/Galvanostat (VersaSTAT-3, Princeton Applied Research) using three-electrode cell and all potentials referred in this work are indicated relative to silver-silver chloride electrode ($Ag/AgCl/Cl^-_{sat.}$) as reference. Working electrode was the test specimen and platinum foil as the counter electrode. The 5% NaCl solution was used as corrosion medium. Potentiodynamic polarization study was carried out in a potential ramp of ±250 mV from open circuit potential (OCP) at scan rate of 1 mVs^{-1}. Corrosion rates were determined by Tafel's extrapolation method and electrochemical impedance study was made in the frequency range from 100 kHz to 20 mHz. The thicknesses of the deposits were calculated from Faradays law. The validity of measured thickness was cross examined using digital thickness tester (Coatmeasure M&C, ISO-17025/2005). The hardness of the deposit (~20μm thickness) was measured by Vickers method using Micro Hardness Tester (CLEMEX). The compositions of the coatings were determined colorimetrically by stripping the deposit into dilute HCl [29]. The cathode current efficiency (CCE) of deposition was determined by knowing the mass and composition of the deposit. The phase structure of the alloys, corresponding to optimum different current densities were analyzed using X-ray Diffractometer (Bruker AXS), using Cu Kα- radiation, (λ=1.5405 A^o, 30 kV). The microstructures of the deposits were examined by Scanning Electron Microscopy (SEM, Model JSM-6380 LA from JEOL, Japan).

3. RESULT AND DISCUSSIONS

3.1. Hull cell study

The bath composition and operating parameters of Zn-Ni, Zn-Co and Zn-Ni-Co baths have been optimized by conventional Hull cell method [30] at 1.0 A cell current, and temperature 300 ^oC. Varieties of deposits having grayish white/bright/mirror bright/porous black appearance were obtained over the wide range of current density of 1.0-5.0 A/dm^2.

Effect of each bath constituents on Hull cell panels were examined in terms of their appearance and surface morphology. The composition and operating parameters of optimal bath is given in Table 1.

Table 1. Composition and operating parameter of optimal bath for electrodeposition of bright Zn-Ni, Zn-Co and Zn-Ni-Co alloy on mild steel

Bath composition(g/L)	Zn-Ni	Zn-Co	Zn-Ni-Co
$ZnSO_4.7H_2O$	120.0	50.0	50.0
$NiSO_4.7H_2O$	100.0	-	100.0
$CoSO_4.7H_2O$	-	15.0	25.0
$C_6H_8O_7.H_2O$	3.0	4.0	4.0
CH_3COONa	70.0	60.0	60.0
$C_{12}H_{17}N_4OSCl.HCl$	0.5	0.5	0.5

3.2. Effect of current density

3.2.1. Wt. % metal in the deposit

The effect of c.d. on wt. Ni% and wt. Co% were studied using optimized bath. It was found that c.d. plays an important role on both appearance and corrosion performance of deposit. Increase of wt. Ni% and Co with increase in current densities and bath follows anomalous codeposition over the entire range of 1.0 A/dm^2 - 5.0 A/dm^2. Both the baths have produced semi bright deposit at low c.d. side and a porous bright deposit at high c.d. The brightness of the deposit was found to be due to THC. The variation of wt. % of M with c.d. in Zn-Ni, Zn-Co and Zn-Ni-Co is as shown in Table 2, 3 and 4.

A sound deposit of Zn-Ni alloy was found at 3.0 A/dm^2 with about 1.9 Ni%. The increase of wt. Ni% in the deposit at low c.d. side is attributed to the tendency of the system to follow normal type with preferential deposition of nickel as shown in Table 2. For the optimized Zn-Co bath wt. Co% obtained in the deposit was varied from 0.39% to 1.08% for different c.d. A sound deposit of Zn-Co alloy was found at 4.0 A/dm^2 with about 1.02% Co in Table 3. A small increase in the wt % of more noble metals was observed in ternary alloy coating with increased corrosion resistance as shown in Table 4. At optimal condition, the Zn-Ni-Co alloy showed 2.9 wt. Ni% and 0.80 wt. Co% (against 1.9 wt. Ni% and 1.02 wt. Co% in Zn-Ni, Zn-Co alloy coatings) in the deposit. It may be observed that a small increase in the noble metal

content in the deposit shows a significant change in the intrinsic electrical properties of the deposit, and hence its corrosion behavior. The CCE% of the bath increased with c.d. to a peak value and then decreased slightly at high c.d. due to hydrogen evolution at the cathode as shown in Table 2, 3 and 4.

Table 2 . Corrosion parameters of Zn-Ni alloy deposits obtained under different current densities using 5% NaCl

c.d (A/dm^2)	wt.% of Ni	CCE (%)	VHN	Thickness (μm)	E_{corr} in Volts Vs.Ag/AgCl	i_{corr} ($\mu Amp/cm^2$)	Corrosion rate $\times 10^{-2}$ (mm/year)
1.0	2.31	92.0	131.5	6.2	-1.242	13.3	19.31
2.0	1.56	93.5	146.5	11.8	-1.241	5.65	8.22
3.0	1.92	94.7	129.5	19.2	-1.286	5.02	7.34
4.0	2.73	92.9	180.5	24.8	-1.224	6.35	9.31
5.0	5.58	94.1	198.6	28.3	-1.316	5.15	9.92

Table 3. Corrosion parameters of Zn-Co alloy deposits obtained under different current densities using 5% NaCl

c.d (A/dm^2)	wt.% of Co	CCE (%)	VHN	Thickness (μm)	E_{corr} in Volts Vs. Ag/AgCl	i_{corr} ($\mu Amp\ cm^{-2}$)	Corrosion rate $\times 10^{-2}$ (mm/year)
1.0	0.39	96.1	152	8.2	-1.295	6.57	9.6
2.0	0.46	97.3	185	10.6	-1.302	5.76	8.5
3.0	0.60	98.6	195	13.5	-1.300	5.22	7.7
4.0	1.02	99.0	259	17.7	-1.233	4.83	7.1
5.0	1.08	93.7	286	20.9	-1.335	5.36	7.8

Table 4. Corrosion parameters of Zn-Ni-Co alloy deposits obtained under different current densities using 5% NaCl

c.d (A/dm^2)	wt.% of Ni	wt.% of Co	CCE (%)	VHN	Thickness (μm)	E_{corr} in Volts Vs. Ag/AgCl	i_{corr} (μAmp cm^{-2})	Corrosion rate$\times10^{-2}$ (mm/year)
1.0	4.3	0.43	95.1	139	7.8	-1.240	1.922	2.82
2.0	2.2	0.61	97.7	158	12.3	-1.212	1.912	2.78
3.0	2.9	0.80	98.0	189	17.5	-1.313	0.274	0.39
4.0	3.8	1.10	97.5	206	22.7	-1.290	1.212	1.76
5.0	7.4	1.20	95.3	198	24.6	-1.254	1.861	2.73

3.2.2. Thickness of deposit

The thickness of the deposit was found to increase significantly with c.d. in Zn-Ni, Zn-Co and Zn-Ni-Co alloys as shown in Table 2, 3 and 4. The linear dependency of thickness with c.d. was found to have influence on composition and appearance of the deposit, as exhibited by any other Zn-Fe group metal alloys.

3.2.3. Hardness of deposit

The hardness of the deposit was found to increase with c.d. in Zn-Ni, Zn-Co and Zn-Ni-Co alloys as shown in Table 2, 3 and 4. It may ascribed by the inherent high density nickel, cobalt (d Zn= 7.14 g cm^{-3} and d Ni = 8.90 g cm^{-3},) in the deposit. But at high c.d., the coating was found to be very thick and hard porous. Thick and porous deposit at very high c.d. is due to metal hydroxide formation caused by rapid evolution of hydrogen during plating.

4. CORROSION STUDY

4.1. Tafel plots

Electroplated specimens were subjected to corrosion study in %5 NaCl solution and experimental data of the Zn-Ni, Zn-Co and Zn-Ni-Co alloys are given in Table 2, 3 and Table 4. Corrosion rate of the deposits were determined by Tafel's extrapolation method. The polarization behavior of Zn-Ni-Co alloy deposited at different c.d. is shown in Fig. 1. It may be observed that at optimal current density of 3.0 A/dm^2, the coating shows least corrosion current, i_{corr} and corrosion rate (CR) of 0.39×10^{-2} mm/year which is about 20 times less

compared to Zn-Ni (7.3×10^{-2} at 3.0 A/dm^2) and 18 times less compared to Zn-Co (7.1×10^{-2} at 4.0 A/dm^2).The relative polarization behavior of Zn-Ni, Zn-Co and Zn-Ni-Co alloys is shown in Fig. 2.

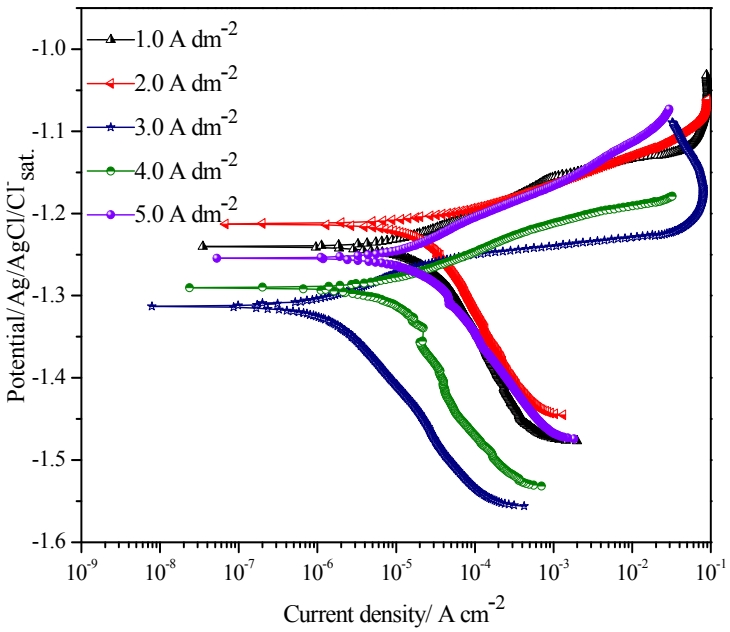

Fig. 1. Tafel plots for Zn-Ni-Co alloy deposits obtained at different current densities from the optimal bath at scan rate of 1 mV/sec vs. Ag/AgCl/Cl$^-_{sat}$

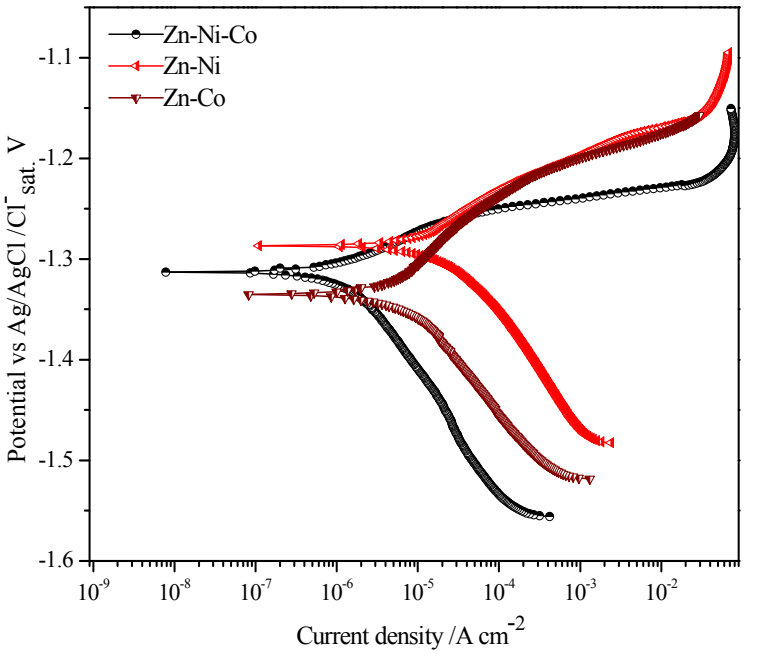

Fig. 2. Tafel plots for Zn-Ni, Zn-Co and Zn-Ni-Co alloy deposits obtained at optimal current densities from the optimal bath at scan rate of 1 mV/sec *vs*. Ag/AgCl/Cl$^-_{sat}$

4.2. EIS study

EIS was used to evaluate the barrier properties of the coatings and to determine the polarization resistance. The superior corrosion resistance Zn-M alloy coatings can be explained by the barrier protection mechanism theory. In this technique, it is common to plot the data as imaginary impedance versus real impedance with provision to distinguish the polarization resistance contribution (Rp) from the solution resistance (Rs). These plots are often called Nyquist diagrams. Nyquist diagrams of Zn-Ni-Co alloy coatings at different current densities were as shown in Fig. 3. Impedance spectra of deposit revealed that improved corrosion resistance of deposit at optimized c.d. is due to improved barrier resistance that is many times higher than that of deposits at other current densities. Fig. 4 shows the impedance signals of the Zn-Ni, Zn-Co and Zn-Ni-Co alloys with very high polarization resistance, (Rp) value in case of ternary alloy.

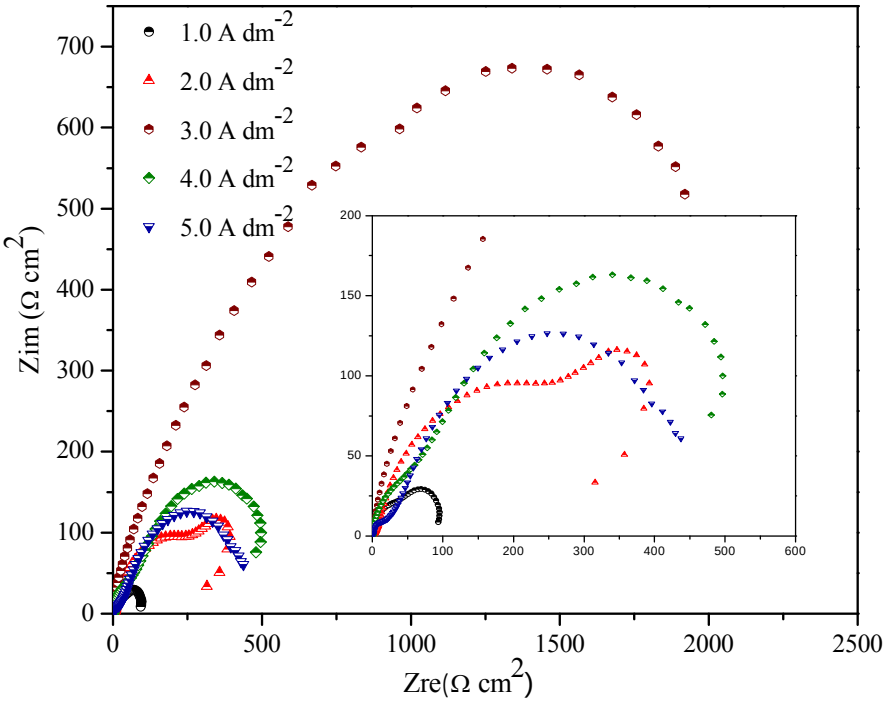

Fig. 3. Electrochemical impedance data display for electrodeposited Zn-Ni-Co coatings from optimal bath at different current densities

4.3. Fitting of impedance data

In EIS, the response of an electrode to alternating potential signals of varying frequency is interpreted on the basis of circuit models of the electrode/electrolyte interface. Consequently Nyquist plot in Fig. 3 can be simulated by the equivalent circuit shown in Fig. 5. Based on the experimental observations, a common electrical equivalent circuit

composed of inductive/ capacitive/resistive elements in series and parallel, with circuit description code LR(C(R)(Q(R(LR)(CR))))) was proposed. Experimental and simulated data fitment was made using built-in software (ZsimpWin 3.21) in the instrument. It is seen that there is a good compatibility between the experimental and simulated data. A best agreement was obtained when a constant phase element was used instead of a pure capacitance, as shown in Fig. 5**.**

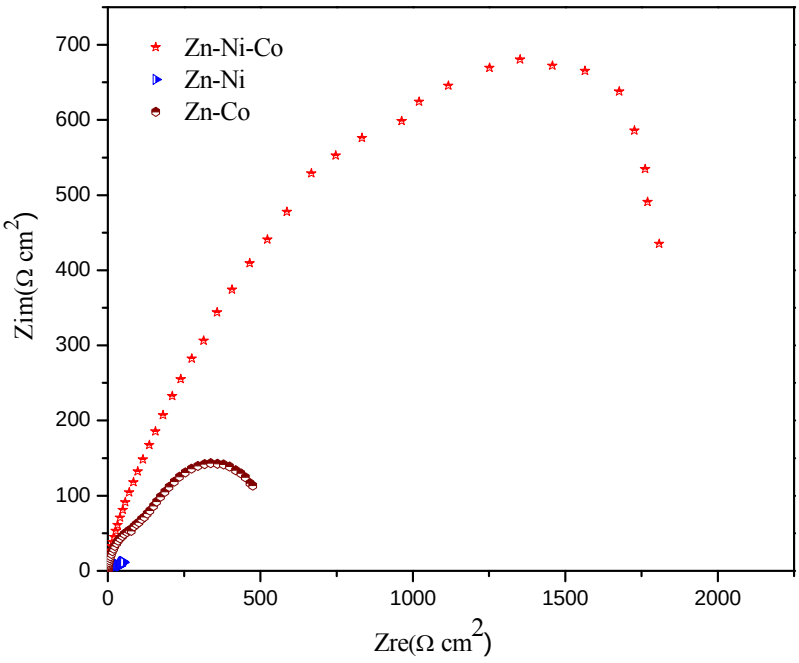

Fig. 4. Electrochemical Impedance spectra of Zn-Ni, Zn-Co and Zn-Ni-Co alloy coatings obtained at optimal current densities from the optimal bath

4.4. Effect of partial current densities on the deposit

Zn-Ni-Co bath produced semi-bright deposits at low c.d. and porous bright deposits at high c.d. A sound deposit of Zn-Ni-Co alloy containing 2.9 wt. Ni% and 0.80 wt. % of Co was obtained at i = 3.0 A/dm^2. The partial deposition current densities were calculated from the mass gained and the chemical composition of the deposit, using the equation**:**

$$i_i = \frac{w}{At} \times \frac{c_i n_i F}{M_i}$$

Where i_i is the partial current density of element i (A/cm^2), w is the weight of the deposit. A is the surface area of the cathode (cm^2). t is the time of deposition. C_i is the weight fraction of the element in the alloy deposit, ni is the number of electrons transferred per atom of each metal, F is the Faraday's constant. M_i is the atomic mass of that element. Fig. 6 shows the dependence of the partial current densities of Zn, Ni and Co on the applied current density.

The partial current densities increased as the applied c.d. was increased. It is also evident that in Zn-Ni-Co alloy system the partial c.d. of Zn is higher than those of the Ni and Co. This supports the possibility of a synergistic catalytic effect of Zn-Ni-Co alloy and vice versa .

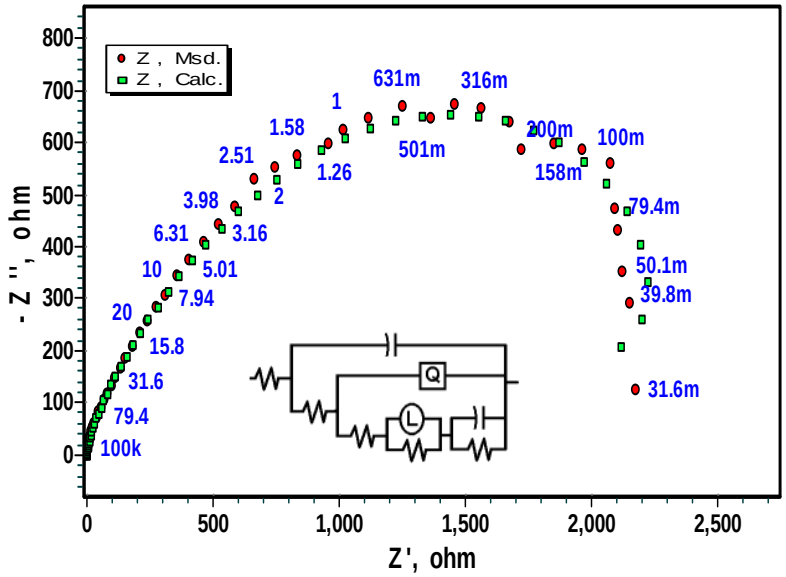

Fig. 5. Equivalent circuit model proposed for electrochemical Impedance spectra of Zn-Ni-Co alloy coatings obtained at optimal c.d. of 3.0 A/dm^2. Model: LR(C(R) (Q(R (LR) (CR)))))

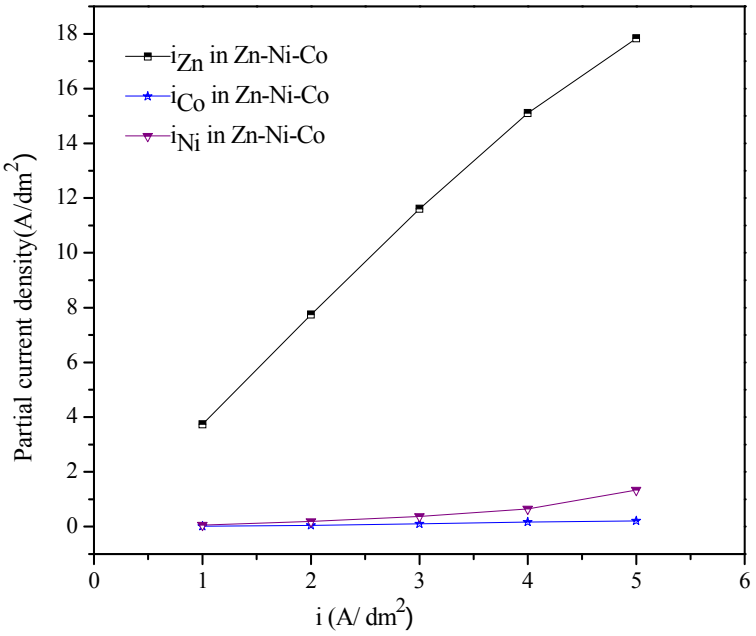

Fig. 6. The dependence of the partial current densities of Zn, Ni and Co on the applied c.d.

4.5. Surface study

The microstructure of deposits, observed by SEM, difference in the uniformity was observed with the increase in the quantity of more noble metal. Fig. 7(a) and 7(b) shows the surface morphology of the Zn-Ni and Zn-Co deposits as observed by SEM. Fig. 7(a) the morphology of the deposits with low nickel content (1.9 wt. Ni%) is granular and isotropic in shape. Similar type of morphology was observed for Zn-Co deposit with the low Co (1.06 wt. Co%) content. Fig. 7(c) shows the SEM image of ternary Zn-Ni-Co deposit. A smooth non granular uniform deposit was observed for Zn-Ni-Co alloy deposit, which is due to the more noble metal in the deposit. EDX analysis was carried out to investigate the metal percentage in the deposit and confirmed the composition of the alloys, and obtained through colorimetric method.

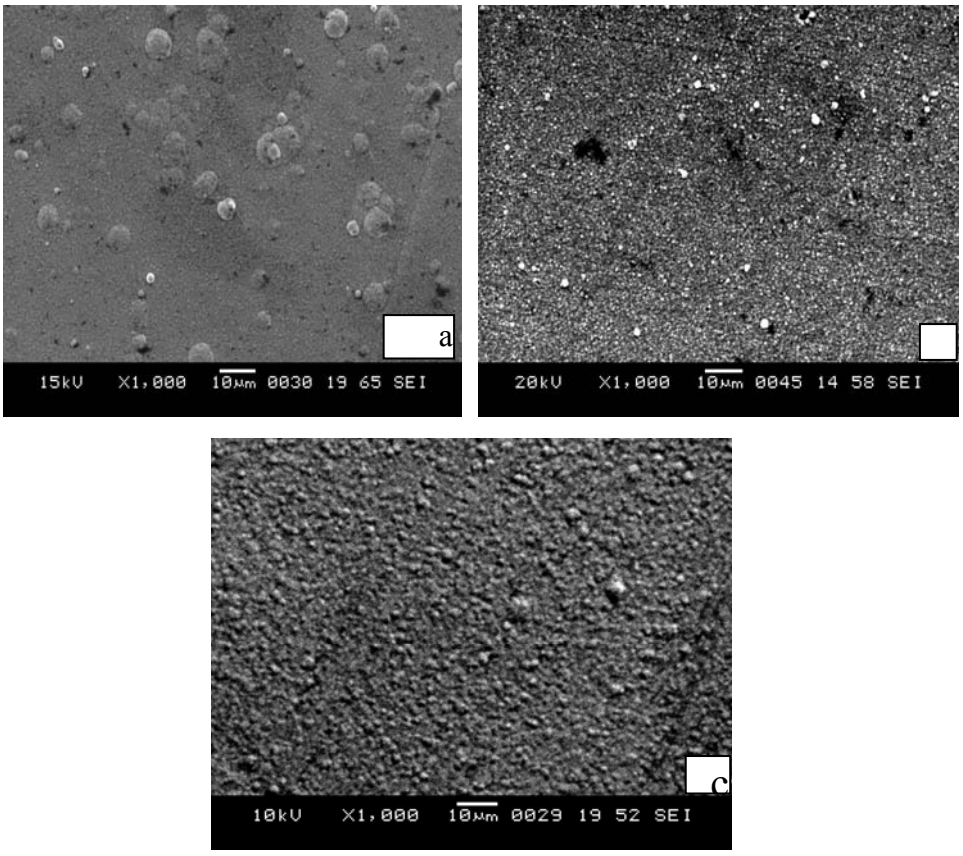

Fig. 7. SEM image of Zn-Ni, Zn-Co and Zn-Ni-Co deposit at optimal current densities (a) 3.0 A/dm^2, (b) 4.0 A/dm^2 and (c) 3.0 A/dm^2

4.6. X-Ray Diffraction Study

Fig. 8 shows the XRD spectra for Zn-Co, Zn-Ni and Zn-Ni-Co coatings on mild steel. The Zn (110) reflection was the highest of zinc, in Zn-Co and Zn-Ni coating indicating preferred orientation of this phase [31]. The spectrum of the Zn-Ni-Co coating was much different. The intensity of Zn (101) became the strongest of Zn. This indicates change in phase content could be reflected by the different appearance in the SEM images (Fig. 7). It may be observed that the intensity of the peak corresponding Zn (100) and Zn (110), Zn (101) increases progressively in binary and ternary alloy coatings at optimized c.d. Thus X-ray diffraction study clearly indicates that a drastic change in corrosion resistance of Zn-Ni-Co coating is the consequent of change in the phase structures of the coatings**.**

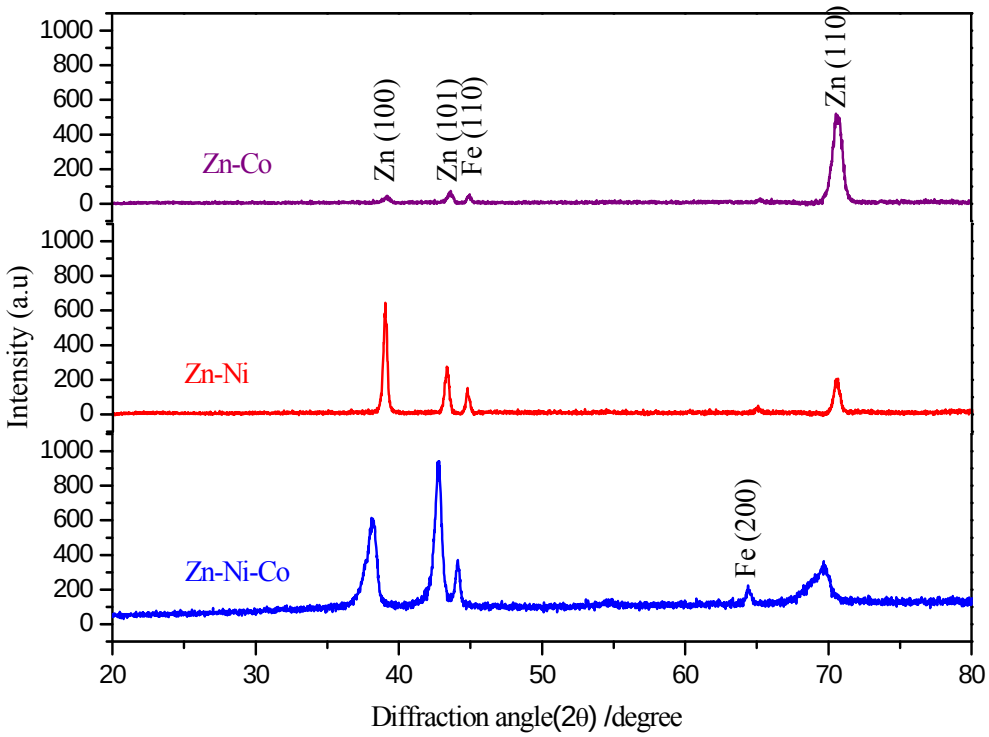

Fig. 8. X-ray diffraction profiles of electrodeposits obtained on mild steel from optimized bath at optimal current densities, as mentioned on the plot

5. CONCLUSIONS

The stable Zn-Ni, Zn-Co and Zn-Ni-Co baths have been proposed. Under worked conditions, the bath followed anomalous codeposition with preferential deposition of less noble metal. Zn-Ni-Co alloy at the c.d. of 3.0 A/dm^2 with 2.9 Ni and % 0.80 Co showed least corrosion rate of 0.39×10^{-2} mm/year, which is about ~20 times less compared to Zn-Ni (7.34×10^{-2} at 3.0 A/dm^2) and ~18 times less in case of Zn-Co (7.1×10^{-2} at 4.0 A/dm^2) alloy.

High partial c.d. for zinc in Zn-Ni-Co alloy system supports the possibility of a synergistic catalytic effect of Ni on Co and vice versa. The polarization studies and electrochemical impedance spectroscopy analysis revealed that superior corrosion resistance of Zn-Ni-Co coatings is due to barrier resistance that is many times higher than that of Zn-Ni and Zn-Co alloys. The SEM images of electroplates confirmed that superior corrosion resistance is due to improved homogeneity of the deposits. The structural and electronic properties of passive layers developed under optimized bath condition are responsible for significant influence on the corrosion behavior of the alloy deposits. More increase of partial current density for Zn compared to Ni and Co, in case of Zn-Ni-Co alloy, indicates the possibility of a synergistic catalytic effect of noble metals. X-ray diffraction study clearly indicates that a drastic change in corrosion resistance of Zn-Ni-Co coating is the consequent of change in the phase structures of the coatings.

REFERENCES

[1] N. Eliaz, E. Gileadi, and C. G. Vayenas, (Ed.), Modern Aspects of Electrochemistry, Springer, New York (2008).
[2] R. Fratesi, G. Roventi, G. Giuliani, and C. R. Tomachuk, J. Appl. Electrochem. 27 (1997) 1088.
[3] Z. L. Wang, Y. X. Yang, and Y. R. Chen, J. Corros. Sci. Eng. 7 (2005) 18.
[4] A. B. Velichenko, J. Portillo, X. Alcobe, M. Sarret, and C. Müller, Electrochim. Acta 46 (2000) 407.
[5] T. V. Byk, T. V. Gaevskaya, and L. S. Tsybulskaya, Surf. Coat. Technol. 202 (2008) 5817.
[6] M. S. Chandrasekar, S. Srinivasan, and M. Pushpavanam, J. Solid State Electrochem. 13 (2009) 781.
[7] M. Sider, C. Fan, and D. L. Piron, J. Appl. Electrochem. 31 (2001) 313.
[8] D. E. Hall, Plat. Surf. Finish. 70 (1983) 59.
[9] R. Ramanauskas, L. Gudaviciute, A. Kalinicenko, and R. Juskėnas, J. Solid State Electrochem. 9 (2005) 900.
[10] J. B. Bajat, S. Stankovic, and B. M. Jokić, J. Solid State Electrochem. 13 (2009) 755.
[11] M. M. Younan, J. Appl. Electrochem. 30 (2000) 55.
[12] J. B. Bajat, A. B. Petrović, and M. D. Maksimovć, J. Serb. Chem. Soc. 70 (2005) 1427.
[13] C. Muller, M. Sarret, and M. Benballa, J. Electrochim. Acta 46 (2001) 2811.
[14] L. Anicai, M. Siteavu, and E. Grunwald, Corros. Prev. Control. 39 (1992) 89.
[15] J. A. Dini, and H. R. Johnson, Met. Finish. 77 (1979) 53.
[16] P. Y. Chen, and I. W. Sun, Electrochim. Acta 46 (2001) 1169.

[17] S. Swathirajan, J. Electroanal. Chem. 221 (1987) 211.
[18] A. Stakeviciute, K. Leinartas, G. Bikulcius, D. Virbalyte, A. Sudavicius, and E. Juzelunas, J. Appl. Electrochem. 28 (1998) 89.
[19] S. M. Rashwan, A. E. Mohamed, S. M. Abd El-Wahaab, and M. M. Kamel, J. Appl. Electrochem. 33 (2003) 1035.
[20] L. Felloni, R. Fratesi, E.Quadrini, and G. Roventi, J. Appl. Electrochem. 7 (1987) 574.
[21] R. Albalat, E. Gómez, C. Müller, M. Sarret, E. Vallés, and J. Pregonas, J. Appl. Electrochem. 20 (1990) 635.
[22] M. M. Younan, and T. Oki, J. Appl. Electrochem. 26 (1996) 537.
[23] H. Bai, and F. Wang, J. Mater. Sci. Technol. 23 (2007) 4.
[24] M. M. Abou-Krisha, H. M. Rageh, and E. A. Matter, Surf. Coat. Technol. 202 (2008) 3739.
[25] K. R. Baldwin, and C. J. E. Smith, Trans. Inst. Met. Finish. 74 (1996) 202.
[26] H. Kim, B. N. Popov, and K. S. Chen, J. Electrochem. Soc. 150 (2003) C81.
[27] L. Felloni, R. Fratesi, E. Quadrini, and G. Roventi, J. Appl. Electrochem. 17 (1987) 574.
[28] A. Brenner, Electrodeposition of Alloys, Vol. II, Academic Press, New York (1963).
[29] A. I. Vogel, Quantitative Inorganic Analysis, Longmans Green and Co London (1951).
[30] Pardhasaradhy, Practical Electroplating Hand Book, Prentice Hall Incl. Pub, Chapter. 3 (1987).
[31] N. Eliaz, K. Venkatakrishna, and A. Chitharanjan Hegde, Surf. Coat. Technol. 205 (2010) 1969.